J Mater Sci (2007) 42:8844–8852
DOI 10.1007/s10853-007-1820-6

NANO- AND MICROMECHANICAL PROPERTIES OF HIERARCHICAL BIOLOGICAL MATERIALS

# Atomistic-mesoscale coupled mechanical analysis of polymeric nanofibers

**V. U. Unnikrishnan · G. U. Unnikrishnan ·
J. N. Reddy · C. T. Lim**

Received: 9 February 2007 / Accepted: 3 May 2007 / Published online: 14 July 2007
© Springer Science+Business Media, LLC 2007

**Abstract** Theoretical analysis of Poly-(L)-Lactic Acid (PLLA) nanofibers is a necessary step towards designing novel biomedical applications. This paper aims to analyze the mechanical properties of PLLA nanofibers so that optimal scaffolds in tissue engineering applications can be developed. We carry out analysis of PLLA nanofibers to estimate the mechanical properties from basic building blocks to the nanofibrous structures. A single PLLA nanofiber is made up of Shish–Kebab like fibrils intertwined together and can contain both amorphous and crystalline phases. The elastic modulus of the Lactic acid monomeric formation in the crystalline phase is derived using second-derivative of the strain energy using molecular dynamics simulation. The mechanical property of the Shish–Kebab fibril is derived by homogenization. The fiber modulus is then obtained using the Northolt and van der Hout's continuous chain theory. One of the significant contributions in this paper is the use of modified continuous chain theory, where a combined multiscale approach is used in the estimation of the mechanical properties of PLLA nanofibers. The theoretical results correlate well with reported experimental data.

## Introduction

Polymeric nanofibers are attractive materials for a wide range of applications in the bio-medical, textile and other emerging technologies. This is primarily due to their large surface area to volume ratio and the unique features at the nanometer scale [1]. Structures of fibrous polymers are generally very flexible, and their conformation is easily deformed against mechanical extension or induced motion between its atoms. In any industrial application, the suitability of a material and/or structure relies significantly on their physical properties, especially their mechanical and electrical properties. Whilst the mechanical design ensures dimensional stability and structural integrity, the electrical design aims to fulfill the functionality of the products.

In recent years, polymeric nanofibers have been developed for a variety of applications such as tissue engineering, molecular filters, sensors and protective clothing [2–6]. For example, polymeric nanofibers can be used to form nanofibrous scaffolds for tissue engineering application [7]. These polymeric scaffolds allow cells to proliferate and grow into tissues with defined sizes and shapes for transplantation purposes [8, 9]. An understanding of the structure–property relationship is essential for the engineering applications of polymeric nanofibers since they are affected by the mechanical properties arising from the internal molecular structures. Tremendous savings in cost can be achieved if preliminary experimental designs can be evaluated theoretically to eliminate inferior designs and reduce

V. U. Unnikrishnan · G. U. Unnikrishnan ·
J. N. Reddy
Advanced Computational Mechanics Laboratory,
Department of Mechanical Engineering, Texas A&M University,
College Station, TX 77843-3123, USA

J. N. Reddy (✉)
Engineering Science Programme,
National University of Singapore, Singapore, Singapore
e-mail: jnreddy@tamu.edu

C. T. Lim (✉)
Division of Bioengineering & Department of Mechanical
Engineering, National University of Singapore,
9 Engineering Drive 1, Singapore 117576, Singapore
e-mail: ctlim@nus.edu.sg

the number of experiments. The proposed theoretical work in the analysis of nanofiber is primarily aimed at providing a computational framework for the estimation of the mechanical properties and to provide a strong connection between experimental observations and theoretical analysis.

Fibers prepared from polymer solution or melt by conventional methods (melt, dry and wet spinning) have diameters in the range of 5–500 mm [10]. Recently, there has been increased interest in the fabrication of nanofibers (with diameters in the range from tens to hundreds of nanometers) using electrospinning [1, 10, 11] for mechanical characterization studies. Using molecular dynamics (MD) simulation, crystalline lactic acid monomer units are equilibrated and thermostatted to the experimental conditions by a series of NVE ensemble (Microcanonical ensemble) and NVT ensemble (Canonical ensemble) analysis and subjected to isothermal strain conditions to obtain the mechanical properties [12, 13]. To develop an optimal scaffold for tissue engineering application, it is required to manipulate the mechanical characteristics of the nanofibrous scaffolds. There has been numerous experimental studies on the design of optimal scaffolds [8]. However, very few theoretical studies exist in predicting the mechanical properties and behavior of nanofibers under external mechanical loads using multiscale simulation. This paper aims to analyze the mechanical properties of PLLA nanofibers via an atomistic-mesoscale stimulation method. All molecular dynamics simulations were performed using Cerius$^2$ (version 4.6, Accelrys, Inc.) simulation package.

Analysis of the orientation process during uniaxial drawing of a polymer has long been investigated in many theoretical and experimental studies [7, 14, 15]. Based on the deformation of cellulose fibers, analytical models were developed for rodlets connected by crosslinks. These models were modified with the various additions like crosslinking with forces applied to the ends of the chains as well as changes in material properties. This research lead to two different formulations for the analysis of polymeric chains: the rubber elasticity theory based on complex constitutive relations and the orientation based mechanism for the analysis of semi-crystalline polymers leading to the aggregate model [16]. The fibrils in a nanofibrous material are found to intertwine to form polymeric nanofibers. The fiber modulus is obtained using the Northolt and van der Hout's continuous chain theory [14, 17–20]. This is an enhancement over conventional homogenization techniques, because the effect of shear deformation of the fibrils is not taken into consideration. The continuum chain formulation used in this paper gives relationships between the macroscopic elastic constants and the orientation parameters based on the spatial distribution of the nanofibrils.

The paper is organized as follows. Section (Atomistic simulation) describes the atomistic simulation of crystalline lactic acid using MD simulation for the estimation of the mechanical properties in the atomistic scale. Homogenization and description of the Shish–Kebab model is discussed in section (Shish–Kebab model—electrospun nanofibers). The multiscale transfer of quantities of interest from the atomistic scale to the mesoscale by micromechanical methods is discussed in sections (Micromechanical analysis) and (Continuum volume averaging: micromechanical method). In section (Continuous chain model of polymeric fibers), the formulation of the continuum chain model to scaleup the material properties is discussed. Section (Results and discussion) combines the results from various methods and finally the paper concludes with a summary in section (Conclusion).

## Atomistic simulation

The knowledge of structure and molecular motion in polymers is essential to understand the properties of practical interest. Theoretical simulation of the physical processes forms the first step in this work. The estimation of the mechanical properties of the PLLA fibers needs to be carried out. There are various methods of estimating the physical properties of atomistic structures, molecular dynamics (MD) simulation being one of them and is used here. Molecular dynamics has been a very popular tool for the determination of mechanical, thermal and other properties of interest in atomistic structures [21–25]. The starting point of a MD simulation is the non-relativistic quantum mechanical time dependent Schrödinger equation. The thermodynamic state characterized by the fixed number of atoms, volume and temperature called the canonical ensemble [25] forms the basis of the MD simulation here. The simulated system and the heat bath couple to form a composite system. The conservation of the energy still holds in the composite system but the total energy of the simulated system fluctuates. The motion of the particles in the system is governed by the Hamiltonian, which is a function of the position and momentum of the particles [13, 25]. The Hamiltonian representing the total energy of an isolated system is given as the sum of the potential and kinetic energy terms and thermodynamic terms, as given by

$$\begin{aligned} \mathrm{H}(r^N, p^N) &= \frac{1}{2m}\sum_i p_i^2 + U(r^N) \\ E(p^N, r^N) &= E_k(p^N) + U(r^N) \end{aligned} \tag{1}$$

where $U(r^N)$ is the potential energy from intermolecular interactions as a function of the spatial ordinate $r^N, \frac{1}{2m}\sum p_i^2$ is the kinetic energy, which represents the momentum $\dot{p}_i$ of the particle $i$ with mass $m_i$ and $p_i$ is a function of the absolute temperature. The time derivative of the Hamiltonian gives

$$\frac{d\mathrm{H}}{dt} = \frac{1}{m}\sum_i p_i \cdot \dot{p}_i + \sum_i \frac{\partial U}{\partial r_i} \cdot \dot{r}_i = 0 \tag{2}$$

and the spatial derivative of the Hamiltonian gives the equation of motion as

$$\frac{d\mathrm{H}}{dr_i} = \frac{\partial U}{\partial r_i} \tag{3}$$

The reliability of a MD simulation depends mainly on the type of potential functions used. The total potential of the computational unit cell is given by the sum of valence bond energies and the nonbonding interactions

$$U^{\mathrm{tot}} = \sum_j \sum_{j>i} \left[ V_{ij}^{B} + V_{ij}^{NB} \right] \tag{4}$$

where $V_{ij}^{B}$ is the potential energy due to bonding and $V_{ij}^{NB}$ is the potential energy due to nonbonding interactions. The force of attraction and repulsion ($F_{\alpha\beta}$) experienced by each molecule is obtained from the gradient of the potential field

$$F_{\alpha\beta} = -\frac{\partial U^{\mathrm{tot}}}{\partial r_{\alpha\beta}} \tag{5}$$

This force is used in calculating the updated position of the atoms and is carried out by the Velocity-Verlet time integration scheme [13]. In this analysis, the time step is chosen in such a way that the material reaches a metastable state at a given ambient temperature. This is normally in the range of femtoseconds ($10^{-15}$ s), and the local variation of the velocity and the kinetic energy about a small increment in time is very small. It has been shown that without a sudden change in the ambient conditions, the molecules vibrate about the mean energy position, which ensures that there is no change in the inherent temperature of the material. At the beginning of each time step of the simulation, updated velocities $v_i\,(t)$ are calculated for each particle by

$$v_i\left(t + \frac{\Delta t}{2}\right) = v_i\left(t - \frac{\Delta t}{2}\right) + \frac{f_i(t)}{m_i}\Delta t \tag{6}$$

where $\Delta t$ is the time step in the MD simulation, $f_i(t)$ is the total force acting on particle $i$ at time $t$ and $m_i$ is the mass of the particle. The coordinates of the particles $r_i(t)$ are updated from the velocities

$$r_i(t + \Delta t) = r_i(t) + v_i(t + \frac{\Delta t}{2})\Delta t \tag{7}$$

From the updated particle position, the interatomic forces are computed from the first derivatives of the potential energy field $E$ with respect to the atomic coordinates $r_{\mathrm{i}}$

$$f_i(t + \Delta t) = \left(\frac{\partial E}{\partial r_i}\right)_{(t+\Delta t)} \tag{8}$$

The elastic constants can be obtained directly from the variation of the potential for nanofibers [13, 23, 26]. The total potential energy due to the strain which is the elastic strain energy can be expanded as a Taylor series for small displacements, with the initial position being represented by the equillibrium position. The elastic moduli tensor can be written as

$$C_{\alpha\beta\gamma\delta} = \frac{1}{2N\Omega_a}\sum_{j\neq i}\left[\left(\frac{d^2U}{dr_{ij}^2} - \frac{1}{r_{ij}}\frac{dU}{dr_{ij}}\right)a_{ij}^{\alpha}a_{ij}^{\beta}a_{ij}^{\gamma}a_{ij}^{\delta} + \delta_{\beta\delta}\underbrace{\frac{1}{r_{ij}}\frac{dU}{dr_{ij}}a_{ij}^{\alpha}a_{ij}^{\gamma}}_{A_{\alpha\gamma}=0}\right] \tag{9}$$

Here $C_{\alpha\beta\gamma\delta}$ is the elastic moduli; $U = U(r_{ij})$ is the potential energy as a function of the interatomic distance $r_{ij}$; $A_{\alpha\gamma}$ is the internal stress tensor, which at equilibrium is equal to zero; $\Omega_a$ is the average volume of an atom; $N$ is the number of atoms; $\delta_{\alpha\beta}$ is the Dirac-Delta function; $\alpha, \beta, \gamma, \delta$ are the spatial dimensions and $a_{ij}^{\alpha}$ is the undeformed value of $r_{ij}$ in the $\alpha$ -direction. The deformation distance is given by $u_{ij}^{\alpha} = r_{ij} - a_{ij}^{\alpha}$ and it is related to the strain by $u_{ij}^{\beta} = a_{ij}^{\alpha}\varepsilon_{\alpha\beta}$where $\varepsilon_{\alpha\beta}$ are the components of the homogenous infinitesimal strain tensor associated with atoms $i$ and $j$.

The knowledge of structure and molecular motion in polymers is essential to the understanding of mechanical and thermal properties. The crystallization behavior of PLLA shows that it is a semicrystalline polymer that crystallizes from melt and from solution to form fibers [27]. Studies on crystal structure of lactide copolymers by various studies have shown that the unit cell of PLLA is a pseudo-orthorhombic structure ($a = 10.6$ Å, $b = 6.1$ Å, and $c = 28.8$ Å), which is used here [28–31]. X-ray diffraction experiments and Nuclear Magnetic Resonance (NMR) analysis for the estimation of the fibrous and crystal structure of PLLA has shown that the crystalline structure of PLLA differs slightly [31] from that used by Hoogsteen et al. [28] and De Santis et al. [29]. However, these differences are not high enough to cause a change in the properties of the PLLA structure. MD analysis of crystalline PLLA is carried out with the crystal structure and the entire computational model is equilibrated to the experimental conditions (see Fig. 1). The minimum energy condition is the starting point for the thermostating analysis, where the crystal structure is analyzed under the influence of thermal energies. Isothermal strain conditions were applied to the thermally equilibrated unit cell and the elastic constants were obtained using second derivative elastic constant analysis [13, 32].

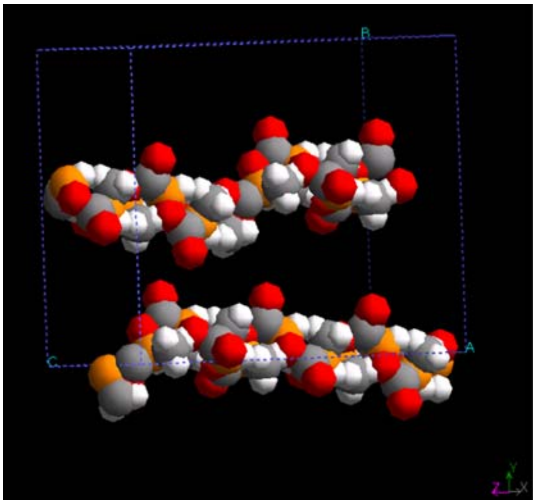

**Fig. 1** Computational domain of the Crystalline PLLA Unit cell

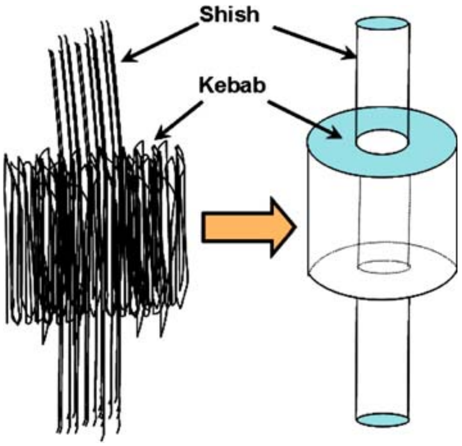

**Fig. 2** Shish–Kebab model and the homogenized equivalent continuum (EC) Shish–Kebab model

### Shish–Kebab model—electrospun nanofibers

Orientation and extension of molecules in a polymer melt affects the crystallization kinetics, structure and morphology. In an entangled polymer, one of the most common crystallization formations is the Shish–Kebab structure [33–35]. The innermost portion of a Shish–Kebab structure is a long and macroscopically smooth extended chain which is crystalline in nature, called a Shish. The Kebabs are folded chain crystalline structures entangling the Shish. The direction of growth of the Kebab is normal to the Shish [12]. There are various views on the formation of the Shish–Kebab structure in a crystallization process; however, in this study we are interested only in the experimentally observed Shish structures in some of the very latest works on crystalline PLLA nanofibers. Shish–Kebab structure can be found in many of the crystallization inducing processes like electro-spinning, melt spinning, etc. [11, 15, 36].

For the polymeric nanofiber, AFM imaging also reveals a "Shish–Kebab" structure [35, 36]. The elastic property obtained from MD analysis is used in the homogenization of the Shish–Kebab model. In this work, we are proposing the homogenization of the Shish–Kebab model assuming that the homogenized axial modulus of Shish is obtained from the crystalline modulus using MD simulations and the Kebab modulus is obtained from the average of the modulus of the RVE in all the directions (see Fig. 2). This assumption is valid since the Shish–Kebab model consists of only crystalline formations.

### Micromechanical analysis

Direct application of the micromechanical methods for the nanofiber raises several questions. Volume averaging of the constituent properties is an established method of bridging the scales [13] and it forms the preliminary basis of multiscale modeling. Here, we deal with the volume averaging of the different elastic measures in the molecular level drawing similarity between the macroscopic quantities, connected by the equivalence of the strain energy due to deformation and the change in the potential energy in an isothermal mechanical straining process. For an elastic composite material, the effective constitutive relations are given by the volume average of the stress and strain. Similarly, for each phase on the micro- and nanoscale, the constitutive relation can be given as

$$\langle\sigma\rangle^k_{\mathrm{tot}} = C^k\langle\varepsilon\rangle^k_{\mathrm{tot}} \tag{10}$$

$\langle\cdot\rangle^k_{\mathrm{tot}}$ is the volume averaged state of phase $k$, including the matrix, fiber and any interphase layers [13]. The volume averaging of the state variables are given by

$$\left\langle\bar{\sigma}_{\alpha\beta}\right\rangle_{EC} = \frac{1}{V}\int\limits_{\Omega}\sigma_{\alpha\beta}dv;\ \left\langle\bar{\varepsilon}_{\alpha\beta}\right\rangle_{EC} = \frac{1}{V}\int\limits_{\Omega}\varepsilon_{\alpha\beta}dv \tag{11}$$

$$\left\langle\bar{\sigma}_{\alpha\beta}\right\rangle_{EC} = C\left\langle\bar{\varepsilon}_{\alpha\beta}\right\rangle_{EC}$$

Similarly, for an $N$ particle atomic ensemble

$$\left\langle\bar{\sigma}_{\alpha\beta}\right\rangle = \frac{1}{N}\sum_{i=1}^{N}\sigma_{\alpha\beta};\ \left\langle\bar{\varepsilon}_{\alpha\beta}\right\rangle = \frac{1}{N}\sum_{i=1}^{N}\varepsilon_{\alpha\beta} \tag{12}$$

$$\left\langle\bar{\sigma}_{\alpha\beta}\right\rangle = C\left\langle\bar{\varepsilon}_{\alpha\beta}\right\rangle$$

For a simple EC, the average stresses due to the atomic ensemble is equal to the average stress due to volume averaging, establishing the relationship between the material constants derived from the MD simulation and volume averaging of the state variables for use in the structural homogenization and micromechanical techniques. Structural models have been developed for foams and cellular materials based on a unit cell. Though these models are based on the information that the porosity of the material is above 70%, this method can be used in the present analysis, as there is a large expected range of porosity ($\Phi$) of the polymeric fiber based on experimental studies [13]. The effective modulus ($E^*$) by the structural model is given as [37]

$$\frac{E^*}{E} = 2.3\left(\frac{\sqrt{3}}{2}(1-\Phi)\right)^3 \qquad (13)$$

Another structural-based homogenization procedure for porous material such as foam, called the 3D open cell material model, is from Gibson and Ashby [37]. The effective modulus of the porous material is related to the fiber modulus by [37]

$$\frac{E^*}{E} = (1-\Phi)^2 \qquad (14)$$

According to Thelen et al. [37], the 3D open cell model is based on assumptions of high porosity; and it gives good predictions of modulus for materials with porosities in the range of 10–90%. The nanofibrous materials definitely fall in this range, and therefore, this model can be used in the conservative prediction of the elastic modulus [27, 38, 39]. However, the major drawback of the methods mentioned above is that the actual amount of voids present in the nanofibers is not known for comparing with experimental data. Hence the porosity based methods cannot be used for a reliable estimate of the stiffness of the nanofiber and therefore we need to look at theories that take into consideration both the porosity and orientation of the nanofiber constituents.

## Continuum volume averaging: micromechanical method

Applying the eshelby eigenstrain formulation, the effect of the fiber phase on the matrix stress is captured by means of an averaged strain concentration tensor [13]. The strain concentration tensors for various morphologies of the fiber phase are considered to cause corresponding eigenstrains on the matrix layer. This can be analyzed using the Mori–Tanaka (MT) method, which is detailed below.

Consider an RVE subjected to a homogenous displacement boundary condition that produces a uniform strain $\varepsilon_{ij}^{o}$ in an infinite homogenous material containing an inclusion as shown in Fig. 3. Eshelby has shown that under the above conditions, the ellipsoidal inclusion experiences a uniform eigenstrain $\varepsilon_{ij}^{*}$. By applying the eigenstrain method, the effective modulus of the RVE can be calculated. MT theory was originally concerned with the calculation of internal stress in a matrix containing inclusions with eigenstrains. However, this theory is valid only for cases where the volume fraction of the inclusion is small. The MT method treats the different inclusions as distinct regions and does not take into consideration the geometry [40, 41]. The MT formulation used in this work follows closely with that of Fisher et al. [40]. In a multiphase model (i.e., material with multiple inclusions), as in the case of a void-PLLA RVE, the different regions are represented as distinct cylindrical phases equivalently dispersed in the matrix (see Fig. 4). This model is further used in the study of fiber orientations. To elucidate the expressions for MT method, we assume that the composite is composed of $K$ phases. The stiffness of the matrix is denoted by $C_m$ and the volume fraction of the matrix is denoted by $v_m$. The $k$th phase (or inclusion) has a stiffness of $C_k$ and volume fraction of $v_k$. The dilute strain concentration factor for the $k$th phase, denoted by $A_k^{\text{dil}}$, relates the volume averaged strain in the $k$th inclusion to that of the matrix [40, 41] and it is obtained from

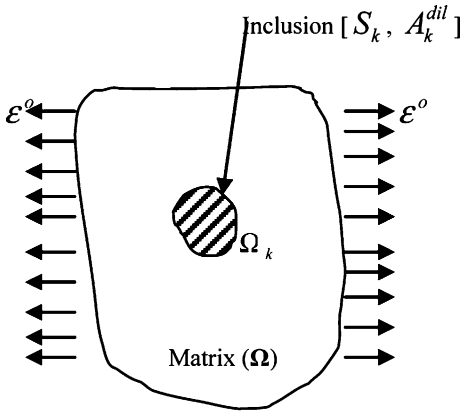

**Fig. 3** Far field strain applied to an RVE with an inclusion

$$\left[S_k + C_m[C_k - C_m]^{-1}\right]A_r^{\text{dil}} - \sum_{n}^{K-1} v_n S_n A_n^{\text{dil}} = -\text{I} \qquad (15)$$

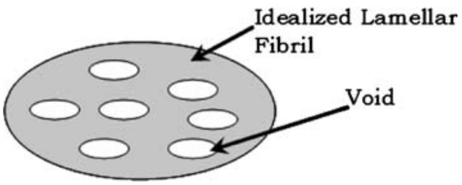

**Fig. 4** Idealized lamellar fibril homogenized model

where $(k,n) = \{f, g, \ldots, K-1\}$, and $S_k$ is the Eshelby Tensor for the dispersed inclusions. The effective modulus of the composite (i.e., matrix with inclusions), $C$, is found from

$$C = C_m \left[ \mathrm{I} - \sum_{k=1}^{K-1} v_k A_k^{\mathrm{dil}} \right] \tag{16}$$

## Continuous chain model of polymeric fibers

Subsequent to the homogenization of the Shish–Kebab model, it is found that a fibril intertwines around other fibrils to form the nanofiber. Tan and Lim [11] have reported that a fibril might terminate by connecting another fibril or it may branch into two others. This type of complex intertwining cannot be modeled by simple homogenization techniques and therefore a detailed analytical procedures need to be considered. The deformation characteristics of an oriented crystalline polymeric fiber have to take into consideration, apart from the mechanical properties of the material, the molecular arrangement in the nanoscale, and at larger length scales [20, 42]. The model that we use in this paper is based on the analysis of extension of oriented crystalline fibers called the continuum chain model. However, we extend this theoretical formulation by incorporating the effect of the smaller-scale material properties by adequate homogenization techniques. It has also been experimentally shown that a polymeric fiber experiences shear deformation when subjected to a tensile test [18]. The elastic deformation of a crystalline fibril is the result of the extension of the chain, which is the predominant effect, and the shear between adjacent chains is the secondary effect [14, 43].

The continuous chain model (series model) developed by Northolt and van der Hout [14, 20, 44] is used for the description of the tensile deformation of the fibers (see Fig. 5). This model describes the deformation of a polymeric fiber as the sum of a linear extension and a rotation of the chains towards the fiber axis. The deformation of the fiber is taken as the average deformation of a polymer chain in the direction of the fiber axis as is shown in Fig. 5. Detailed description of the continuous chain model can be found in Northolt [27], and Northolt and van der Hout [14]. We propose to modify the elastic and shear modulus $(E_c, G_c)$ of the chain used in this model by the homogenized elastic and shear modulus $(E_c(S, v_S, v_k)$, $G_c(S, v_s, v_k))$, which are functions of (1) the Eshelby tensor ($S$) for the circular inclusions, and (2) the volume fraction of the Shish and Kebab $(v_S, v_k)$ or an equivalent homogenized structure. Thus, the effective fiber modulus is obtained by

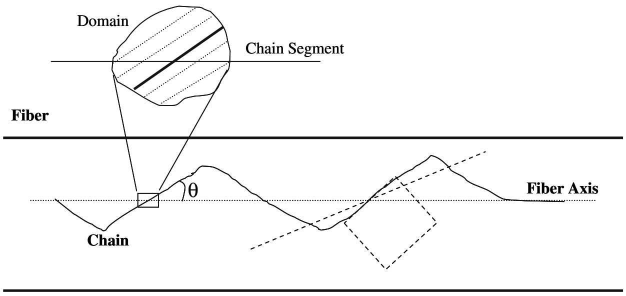

**Fig. 5** Schematics of a chain, a chain segment and the surrounding domain in the analysis using a continuous chain model

$$\frac{1}{E_{\text{fiber}}} = \frac{1}{E_c(S, v_s, v_k)} + \frac{\langle \sin^2\theta \rangle_E}{2G_c(S, v_s, v_k)} \tag{17}$$

where $E_{fiber}$ is the fiber modulus, $\langle \sin^2\theta \rangle_E$ is the strain orientation parameter and is given by the following equation. [14, 17]:

$$\langle \sin^2\theta \rangle_E = \frac{\int_0^{\pi/2} \rho(\theta) \cos\theta \sin^3\theta \, d\theta}{\int_0^{\pi/2} \rho(\theta) \cos\theta \sin\theta \, d\theta} \tag{18}$$

The modified fibril strain can subsequently be written as the sum of the elastic strain and the strain due to elastic rotation or shear of the fibrils as given by

$$\varepsilon_f = \frac{\sigma}{E_f(S, v_s, v_k)} + \frac{\langle \sin^2\theta \rangle_E}{2} \left( 1 - e^{-\frac{\sigma}{G(S, v_s, v_k)}} \right) \tag{19}$$

## Results and discussion

There is a wide range in the reported values of the mechanical properties of PLLA fibers [14, 18–20, 43, 44]. These are primarily affected by various factors like rate of drawing of the polymer, temperature and crystallinity of the polymer material [14, 19, 44]. Most of the studies carried out so far do not take into consideration the porosity of the nanofiber. There have been very few studies on the internal structure of an electrospun nanofibrous material and most of these studies have been aimed at providing the factors affecting the nanofiber dimensions [45, 46]. The mechanical stiffness of the nanofiber obtained by using Timoshenko beam theory and ordinary beam bending theory give conservative values. These results are not reliable since they do not capture the inherent orientation inhomogeneity of the nanofiber. The material modeling strategy used here is novel as it considers the inhomogeneity of the nanofiber and the orientation of the fibrils [7, 11, 15, 36]. This modeling procedure is carried out by using mathematically well-established multiscale modeling simulation techniques coupling the atomistic scale to macroscopic scales. To the best knowledge of the authors, such a methodology of extracting the material properties from a completely computational point of view (independent of experimental data) for nanofibers has not been attempted. As homogenization methods considering only the individual aspects of material modeling at different scales are available in literature, a multiscale computational framework is being proposed in this work. The material properties are extracted from the molecular to the macro level, and finally validated with independent experimental results. The uniqueness is in the multiscale approach proposed here.

High strength PLLA fibers of the order of 16 GPa with high crystallinity and porosity has been produced by dry spinning [38]. Leenslag and Pennings have reported a tensile modulus of 14 GPa for solution-spun PLA fibers [39]. Numerous studies by researchers have produced high modulus PLLA fibers for various uses, having elastic modulus ranging from 1 to 20 GPa. For example, Tan and Lim [36] reported elastic modulus values of 1–10 GPa, Hoogsteen et al. [28] 16 GPa, Yuan et al. [47] 1–5 GPa, Broz et al. [48] 3.0 GPa, and Cicero and Dorgan [49] reported 1.5–3.0 GPa for different draw ratios. Inai et al. [1] reported the elastic modulus in the range of 2.9 ± 0.4 GPa for semi-crystalline electrospun polymeric PLLA fibers. Most of the above reported values were attained by the estimation of elastic stiffness in tension. Flexural modulus in the range of 6–9 GPa was obtained by Lim et al. [50].

The Young's modulus obtained from MD analysis of crystalline lactic acid should conform to the experimental value of the modulus of crystalline PLLA [51]. The experimentally obtained elastic modulus for a ~90% crystalline PLLA made by a hot drawn (melt spinning) process is 9.2 GPa [51] and a Poisson's ratio of 0.44 has been reported by Balac et al. [52]. The MD simulations were performed with a fixed time step of 1 fs and the interatomic interactions were calculated using a Universal 1.02 force field (UFF) of Cerius$^2$ (version 4.6, Accelrys, Inc.) in all the simulations [53]. This potential function includes van der Waals, bond stretch, bond angle bend, and torsional rotation terms. The computational unit cell was minimized and equilibrated by NVE process. The temperature scaling was carried out using NVT ensemble with the Nosé–Hoover thermostat. During the minimization and NVT processes, the atoms are allowed to equilibrate within the fixed MD cell.

An elastic modulus of 9.44 GPa along the major axis, and 5.71 GPa and 4.57 GPa along the minor axes with an average Poisson's ratio of 0.4 was obtained using MD simulations. The resultant effective modulus of the nanofibrous structure obtained using Mori–Tanaka method was 5.77 GPa, by considering about 0.2 volume fraction of the Shish in Kebab in the nanofiber. This obtained effective modulus closely matches with many of the effective properties obtained [28, 36, 50]. The effective modulus of the Shish–Kebab configuration is now used in the modified continuum chain model to obtain the variation of the effective properties of the nanofiber with varying orientation parameter values.

The elastic stiffness calculated using the Mori–Tanaka, 3D open cell and honeycomb structure models is given in Fig. 6. It can be seen that the predicted stiffness values has a maximum of 5.9 GPa and decreases with an increase in porosity. The amount of porosity is also indicative of the diameter of the fiber, as the diameter increases the porosity of the fiber also increases as seen from experimental observations [11]. It can be seen from Fig. 6 that with an increase in diameter the elastic stiffness would decrease. This method, however, fails to provide an accurate estimation of the elastic modulus of nanofibrous materials, when compared to experiments (see, for example, Inai et al. [1]). The average elastic property obtained by homogenization of the Shish–Kebab model is used in the modified continuum chain model. In this continuum chain model, the homogenized elastic property is predicted by Eq. 17 using the strain orientation parameter derived from the birefringence data (Eq. 18). This analytically predicted elastic modulus of PLLA fibers (as shown in Fig. 7) closely matches with the experimental values of Mezghani [54]. The stress-strain curves, using the continuum chain model and the experimentally determined values for different draw velocities by Inai et al. [1] is compared in Fig. 8.

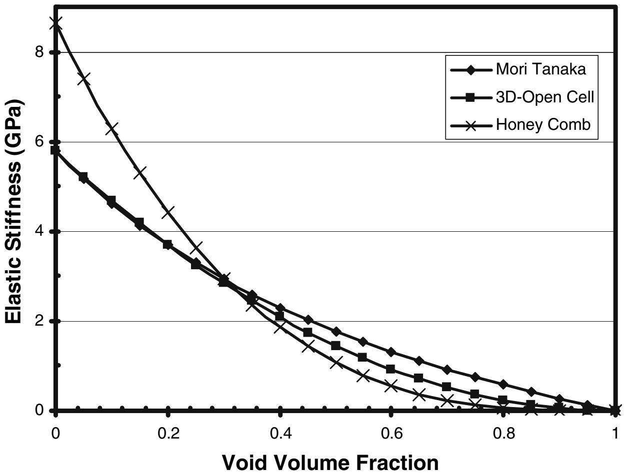

**Fig. 6** Variation of elastic modulus of nanofibers with void volume fractions

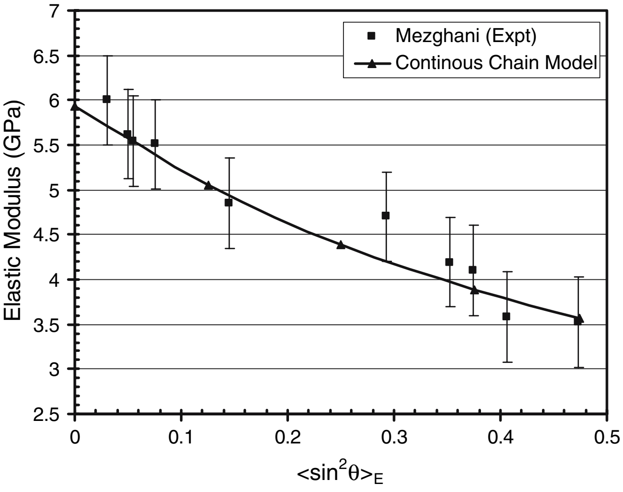

**Fig. 7** Variation of elastic modulus with the strain orientation parameter

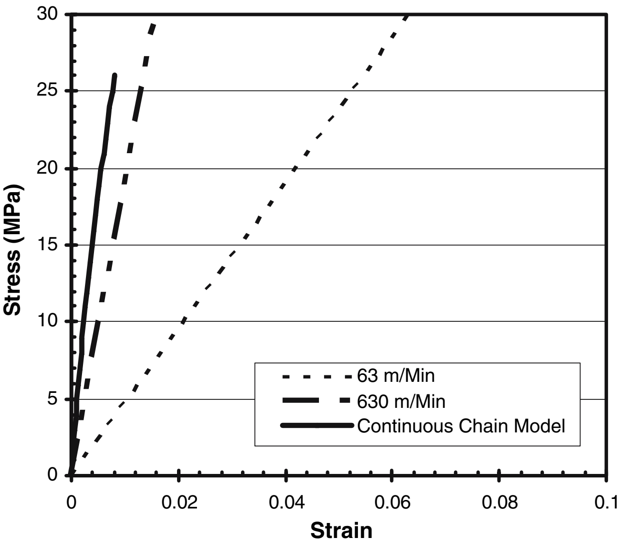

**Fig. 8** Comparison of stress-strain curves with that obtained from experiments

From the figure, it can be seen that the predicted stress-strain curve lies closer to the higher draw velocity curve. The modified continuum chain model predicts a stiffer fiber due to the inadequate information on the internal structure of the nanofiber. With a better understanding of the internal structure a more refined estimate of the stress-strain curve can be obtained.

## Conclusions

In this study, a multiscale modeling approach is used to obtain the effective elastic modulus of the PLLA nanofiber. The analysis is carried out from the atomistic level using MD simulation to obtain the crystalline elastic modulus. The next scale of modeling is the homogenization of the Shish–Kebab model using the Mori–Tanaka method. Based on this homogenization principle, the modified elastic constants are obtained and are subsequently used in the homogenized-continuum chain model to obtain the macroscale homogenized elastic modulus. The highlight here is the multiscale method of estimating the elastic properties of PLLA nanofibers, as compared to previous computational procedures that depend solely on either the conventional continuum chain model or atomistic simulations only. The simulation results obtained show excellent correlation with that of experiments, even without involving any experimental data in the analysis.

**Acknowledgements** The authors would like to acknowledge support of the Laboratory for Molecular Simulation at Texas A&M University for providing software and computer time. The first three authors also gratefully acknowledge the partial support received from Dr. C. F. Shih at the National University of Singapore.

## References

1. Inai R, Kotaki M, Ramakrishna S (2005) Nanotechnology 16:208
2. Lim TC, Kotaki M, Yong TKJ, Yang F, Fujihara K, Ramakrishna S (2004) Mater Technol (Nano Bio-engineering Special) 19:20
3. Lim TC, Ramakrishna S (2005) In: Next-generation applications for polymeric nanofibres. John Wiley, England, p 137
4. Ramakrishna S, Fujihara K, Teo WE, Lim TC, Ma ZW (2005) In: An introduction to electrospinning and nanofibers. World Scientific, Singapore
5. Ramakrishna S, Fujihara K, Ganesh VK, Teo WE, Lim TC (2005) In: Science and engineering of polymer nanofibers. American Scientific Publisher, California
6. Zammaretti P, Jaconi M (2004) Curr Opin Biotechnol 15:430
7. Tan EPS, Lim CT (2006) J Biomed Mat Res— Part A 77A:526
8. Freed LE, Vunjak-Novakovic G, Biron RJ, Eagles DB, Lesnoy DC, Barlow SK, Langer R (1994) Bio/Technology 12:689
9. Moran JM, Pazzano D, Bonassar LJ (2003) Tissue Eng 9:63
10. Lee KH, Kim HY, Khil MS, Ra YM, Lee DR (2003) Polymer 44:1287
11. Tan EPS, Lim CT (2005) Appl Phys Lett 87:123106
12. Dukovski I, Muthukumar M (2003) J Chem Phys 118:6648
13. Unnikrishnan VU, Reddy JN (2005) Int J Multiscale Comput Eng 3:437
14. Northolt MG, Hout RVD (1985) Polymer 26:310
15. Tan EPS, Lim CT (2006) Composites Sci Technol 66:1099
16. Richardson ID, Ward IM (1970) J Phys D: Appl Phys 3:643
17. Northolt MG (1980) Polymer 21:1199
18. Northolt MG, Baltussen JJM (2002) J Appl Polym Sci 83:508
19. Northolt MG, Baltussen JJM (2002) J Appl Polym Sci 83:508
20. Northolt MG, Roos A, Kampschreur JH (1989) J Polym Sci: Part B: Polym Phys 27:1107
21. Frankland SJV, Brenner DW (1999) In: National meeting of the american chemical society. New Orleans, LA, p 38953
22. Qian D, Wagner GJ, Liu WK, Yu MF, Ruoff RS (2002) Appl Mech Rev 55(6):495
23. Chandra N, Namilae S, Shet C (2004) Phys Rev B 69:94101
24. Mylvaganam K, Zhang L (2004) Carbon 42:2025
25. Griebel M, Hamaekers J (2004) Comp Methods Appl Mech Eng 193:1773

26. Blonski S, Brostow W, Kubÿt J (1994) Phys Rev B 49:6494
27. Kalb B, Pennings AJ (1980) Polymer 21:607
28. Hoogsteen W, Postema AR, Pennings AJ, Ten Brinke G (1990) Macromolecules 23:634
29. De-Santis P, Kovacs AJ (1968) Biopolymers 6:299
30. Yamane H, Sasai K, Takano M (2004) J Rheol 48:599
31. Fujita M, Doi Y (2003) Biomacromolecules 4:1301
32. Namilae S, Chandra N, Shet C (2004) Chem Phys Lett 387:247
33. Somania RH, Yanga L, Zhub L, Hsiao BS (2005) Polymer 46:8587
34. Welch P, Muthukumar M (2001) Phys Rev Lett 87:218302
35. Zussman E, Rittel D, Yarin AL (2003) Appl Phys Lett 82:3958
36. Tan EPS, Lim CT (2004) Appl Phys Lett 84:3400
37. Thelen S, Barthelat F, Brinson LC (2004) J Biomed Mat Res 69A:601
38. Leenslag JW, Pennings AJ (1987) Polym Commun 28:92
39. Leenslag JW, Pennings AJ (1987) Polymer 28:1695
40. Fisher FT, Bradshaw RD, Brinson LC (2003) Compo Sci Technol 63(11):1689
41. Mura T (1997) In: Micromechanics of defects in solids. Kluwer Academic
42. Ward IM (1967) Br J Appl Phys 18:1165
43. Baltussen JJM, Northolt MG (2001) Polymer 42:3835
44. Baltussen JJM, Northolt MG, Hout RVD (1997) J Rheol 41:549
45. Ruotsalainen T, Turku J, Heikkilä P, Ruokolainen J, Nykänen A, Laitinen T, Torkkeli M, Serimaa R, Ten Brinke G, Harlin A, Ikkala O (2005) Adv Mater 17:1048
46. Demir MM, Yilgor I, Yilgor E, Erman B (2002) Polymer 43:3303
47. Yuan XY, Mak AFT, Yao KD (2003) Polym Degrad Stability 79(1):45
48. Broz ME, Vander Hart DL, Washburn NR (2003) Biomaterials 24:4181
49. Cicero JA, Dorgan JR (2001) J Polym Environ 9:1
50. Lim JY, Kim SH, Lim S, Kim YH (2002) Macromol Chem Phys 202:2447
51. Fambri L, Pergoretti A, Fenner R, Incardona D, Migliaresi C (1997) Polymer 38:79
52. Balac I, Milovancevic M, Tang C-Y, Uskokovic PS, Uskokovic DP (2004) Mater Lett 58:2437
53. Rappe AK, Casewit CJ, Colwell KS, Goddard WA, Skiff WM (1992) J Am Chem Soc 114:10024
54. Mezghani K, Spruiell JE (1998) J Polym Sci: Part B: Polym Phys 36:1005